Journal of Materials Chemistry A

RSC Publishing

PAPER

View Article Online
View Journal | View Issue

Cite this: *J. Mater. Chem. A*, 2013, **1**, 302

# Scalable synthesis of hollow $Cu_2O$ nanocubes with unique optical properties *via* a simple hydrolysis-based approach†

Hui Liu,[a] Yue Zhou,[a] Sergei A. Kulinich,[b] Jia-Jun Li,[a] Li-Li Han,[a] Shi-Zhang Qiao[ac] and Xi-Wen Du*[a]

Hydrolysis reactions merely involve a precursor and water, which makes them very attractive for the mass-production of nanomaterials at low cost. In the present study, the behavior of cuprous chloride (CuCl) in water solutions was comprehensively investigated, and the medium pH was found to be critical for engineering the reactions and final products. Accordingly, a facile and efficient process based on pH-controlled hydrolysis was designed to fabricate a unique nanostructure, hollow $Cu_2O$ nanocubes. In this process, commercially available CuCl micro-powder is first dissolved in highly acidic water. Then, upon increasing the pH, uniform CuCl nanocubes precipitate and further serve as self-sacrificial templates to produce hollow $Cu_2O$ nanocubes *via* hydrolysis. The synthesis is fast, takes place at room temperature and is solely based on tuning the medium pH. The product exhibits a homogenous size, well-defined shape, surfactant-free surface and excellent optical properties, indicating that hydrolysis-based synthetic routes can be a powerful method for preparing novel nanostructures on a large scale and at low cost.

Received 31st August 2012
Accepted 2nd October 2012

DOI: 10.1039/c2ta00138a

**www.rsc.org/MaterialsA**



## Introduction

Nanostructures with hollow interiors have recently attracted a great deal of attention, as such materials exhibit a number of unique physical and chemical properties.[1–9] For example, they can serve as extremely small containers for encapsulation, which has been extensively applied in catalysis,[10,11] drug delivery[12–15] and ion storage.[16] Furthermore, owing to their high surface area and low density, hollow nanomaterials may possess different properties to their "solid" counterparts.[17] To date, many strategies have been developed to prepare various hollow nanostructures. In general, they can be categorized into four main classes: (i) template-mediated approaches, (ii) chemical etching, (iii) galvanic replacement, and (iv) the Kirkendall voiding.[5,7,18] Among these, template-mediated approaches are the most popular,[18] and the various templates can be in turn classified, according to their role in the synthesis, as hard,[16,19] soft,[20–22] or sacrificial.[23] The latter (*i.e.* the self-sacrificial template) method is regarded as a very simple and attractive method, in which a post-treatment stage, necessary in the hard template method, is avoided, while better control over morphology is achieved compared to that in the soft template approach.

$Cu_2O$ is an environmentally friendly p-type semiconductor with a direct forbidden band gap of ~2.2 eV (ref. 23 and 24) and a high optical absorption coefficient,[25,26] which makes it very favorable for solar energy conversion[23,24,27–29] and photocatalytic applications.[30,31] Because of the above advantages demonstrated by hollow nanostructures, many efforts have been made to obtain hollow $Cu_2O$ nanomaterials. For example, Qi and co-workers synthesized single-crystalline octahedral $Cu_2O$ nanocages *via* a Pd-catalytic reduction of a basic copper tartrate complex solution with glucose followed by an oxygen-engaged catalytic oxidation process.[32] Teo *et al.* prepared hollow $Cu_2O$ nanocubes (NCs) by reducing self-assembled CuO nanocrystals in *N*,*N*-dimethylformamide as a solvent at high temperatures.[33] Yang and co-workers synthesized hollow $Cu_2O$ nanospheres by oxidizing Cu nanoparticles prepared through the thermal decomposition of Cu(I) acetate in trioctylamine in the presence of tetradecylphosphonic acid.[23] Sui *et al.* fabricated hollow $Cu_2O$ nanoframes and nanocages by the oxidative etching of polyhedral $Cu_2O$ particles prepared *via* the reduction of a copper citrate complex with polyvinylpyrrolidone as a capping agent at room temperature for 16 days.[31] More recently, Zhang *et al.* fabricated $Cu_2O$ nanoshells through an Ostwald ripening-based

[a]*Tianjin Key Laboratory of Composite and Functional Materials, School of Materials Science and Engineering, Tianjin University, Tianjin 300072, P. R. China. E-mail: xwdu@tju.edu.cn; Fax: +86 22 87894128; Tel: +86 22 27406794*

[b]*Department of Materials Engineering, Graduate School of Engineering, Osaka University, Suita, Osaka 565-0871, Japan*

[c]*School of Chemical Engineering, University of Adelaide, SA 5005, Australia*

† Electronic supplementary information (ESI) available: SEM and TEM images of the raw CuCl micro-powder used as the initial material, HRTEM image of the shell of a hollow $Cu_2O$ nanocube, calculations of the pH threshold for the complexation of CuCl in aqueous solutions and the lower pH limit for the alkaline hydrolysis of CuCl in aqueous solution, TEM images of the products of reactions between CuCl and water at different pH values, SEM image and XRD pattern of CuCl NCs, XRD patterns of the product after the reaction of CuCl with water (pH 6.5) for different times, FTIR spectrum of RhB and a mixture of hollow $Cu_2O$ NCs and RhB. See DOI: 10.1039/c2ta00138a

symmetric hollowing process in the presence of polyvinylpyrrolidone or polyethylene glycol.[34] However, all the reported synthetic routes are relatively complex, time consuming, and typically involve expensive and/or toxic solvents and surfactants, which makes it difficult to purify the as-produced hollow $Cu_2O$ nanostructure, as well as to scale up such processes.

Hydrolysis reactions have been proved to be facile and efficient for the synthesis of nanomaterials, because they merely involve a precursor and water, and can take place at low temperatures.[35,36] As a potential precursor, CuCl micro-powder is a low-cost and commercially available material which is widely used as a pigment, catalyst, heat and light stabilizer for nylon, desulfuring agent in the refinery industry, and so on.[37,38] It is known to react with water, giving various products, such as $HCuCl_2$, $CuCl_2$, Cu and $Cu_2O$, depending on the pH value of the medium.[39–41] Therefore it can be regarded as a commercially attractive starting material for the synthesis of $Cu_2O$ nanostructures.

In the present study, we carefully investigate the role of the pH value in the reactions of CuCl in water, and design a simple and efficient synthetic route to prepare hollow $Cu_2O$ NCs, solely by adjusting the pH value of the medium. As shown in Scheme 1, CuCl micro-powder is first dissolved in a dilute HCl solution with a low pH value (Scheme 1a and b). Then pure water is added to the solution to raise the pH value, resulting in an immediate precipitation of uniform CuCl NCs (Scheme 1c). Finally, the as-prepared CuCl NCs undergo alkaline hydrolysis and serve as self-sacrificial templates to produce hollow $Cu_2O$ NCs in the same solution (Scheme 1d).

The synthesis uses an inexpensive CuCl micro-powder as a precursor, and proceeds in aqueous medium as a one-pot process at room temperature and with high reaction rates, which makes the as-produced, low cost hollow $Cu_2O$ NCs materials highly attractive for mass production. At the same time, the hydrolysis approach proceeds in the absence of any surfactants, ensuring a very clean product surface, which makes such hollow $Cu_2O$ NCs promising for both further surface functionalization and for use as components in the synthesis of more complex nanostructures. To the best of our knowledge, this is the first report of the synthesis of surfactant-free hollow nanostructures achieved *via* a hydrolysis-based approach at room temperature.

## Results and discussion

CuCl micro-powder was used as a cuprous source. As shown in the SEM image in Fig. S1a,† the raw CuCl micro-particles exhibited an irregular morphology, smooth surfaces, and particle sizes varying from several microns to several tens of microns, which is also illustrated in the TEM image in Fig. S1b.† The X-ray diffraction (XRD) pattern (blue line) in Fig. 1d shows that the precursor material was pure CuCl micro-particles with a cubic crystal structure.

Uniform $Cu_2O$ NCs with particle sizes of about 200 nm were obtained after the CuCl micro-powder was dissolved in aqueous HCl (pH 0.5), and then reacted with water at pH 6.5 for 0.5 h at room temperature (Fig. 1a). As shown in Fig. 1c, nearly all of the NCs are hollow inside and have shells of ~50 nm thickness. In addition, HRTEM analysis of the hollow NCs (see Fig. S2†) revealed their single-crystalline nature.

Below, we discuss the transformation mechanism from CuCl micro-powder to hollow $Cu_2O$ NCs (see Scheme 1) in greater detail. The behavior of CuCl in aqueous solutions is known to be pH sensitive, with the possible reactions including complexation (eqn (1)), disproportionation (eqn (2)), and alkaline hydrolysis (eqn (3)).[39,40]

$$CuCl + xHCl \leftrightarrow H_xCuCl_{1+x} \quad (1)$$

$$2CuCl = CuCl_2 + Cu \quad (2)$$

$$2CuCl + 2OH^- = 2Cl^- + Cu_2O + H_2O \quad (3)$$

Among them, the complexation of CuCl with HCl is known to proceed preferably at low pH values, while the alkaline hydrolysis only takes place at high pH values. The disproportionation (eqn (2)) competes with the other two reactions and becomes dominant at intermediate pH values. However, the pH ranges for the above reactions have not been precisely determined yet. Therefore, we first calculated the pH boundary values for the above reactions (eqn (1)–(3)). The pH boundary between the complexation and disproportionation reactions (eqn (1) and (2)) was determined to be about 2.4, based on the minimum concentration of copper-related species in aqueous HCl (see the details in Section 3 of ESI†). When pH is below 2.4, CuCl

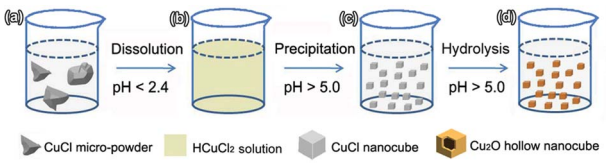


**Scheme 1** Schematic illustration of the one-pot synthetic route from CuCl micro-powder to fine hollow $Cu_2O$ NCs with uniform sizes.

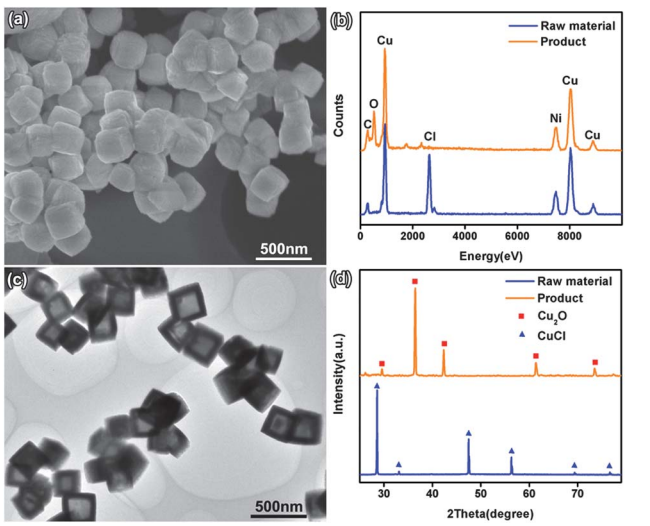


**Fig. 1** (a) SEM image of hollow $Cu_2O$ NCs, (b) EDS spectra of raw CuCl micro-powder and hollow $Cu_2O$ NCs, (c) TEM image of the hollow $Cu_2O$ NCs, (d) XRD patterns of raw CuCl micro-powder and hollow $Cu_2O$ NCs.

dissolves reversibly according to eqn (1). The pH boundary between the disproportionation and the alkaline hydrolysis (eqn (2) and (3)) was determined to be 5.0 based on the saturated solubility of CuCl in water (see the details in Section 4 of ESI†). Correspondingly, the disproportionation reaction (eqn (2)) is concluded to take place within the pH range of 2.4–5.0, giving rise to $CuCl_2$ and Cu. When the pH values are over 5.0, CuCl undergoes alkaline hydrolysis according to eqn (3), which results in the formation of $Cu_2O$.

To verify the above statements, five aqueous solutions with different pH values (10 ml each) were added to 0.1 ml of a saturated solution of CuCl with the pH value of 1.5, and both the color and the absorption spectra of the products were examined (Fig. 2). Upon adding the aqueous solution with a very low pH value (−1.1), a dark yellow solution of $HCuCl_2$ was obtained (see the inset in Fig. 2). As shown by its UV spectrum (Fig. 2), $HCuCl_2$ exhibits an intensive absorption band at wavelengths below 350 nm. After the aqueous solution with the pH value of 2.5 was added, the pH value of the resultant mixture was close to 2.4, which corresponds to the minimum concentration of copper-related species. As a result, CuCl particles precipitated and deposited at the bottom of the cuvette, and the light absorbance of this sample shifted to below 400 nm, which should arise from CuCl (see the inset in Fig. 2). These results suggest that the pH value of 2.4 is indeed the boundary value between the dissolution and precipitation of CuCl (the reversible reaction described by eqn (1)). Upon adding the aqueous solution with a pH value of 4.3, the mixture gradually turned reddish, giving rise to a reddish deposit at the bottom of the container (see the inset in Fig. 2). As shown in the spectrum (red line), the deposit exhibited an absorption peak at around 600 nm, which is typical of the surface plasmon resonance peak of metallic Cu.[42,43] The TEM image in Fig. S3a† also proves that the reddish deposit was composed of Cu nanoparticles, which exhibited a single-crystalline structure in the HRTEM image (Fig. S3b†). These results indicate that the disproportionation reaction (eqn (2)) with the generation of Cu nanoparticles does take place at pH values close to 4.3.

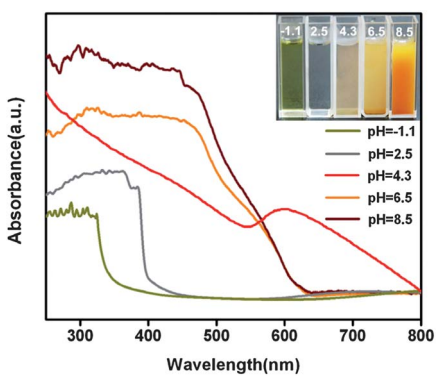


**Fig. 2** Absorption spectra of products obtained by mixing 0.1 ml of saturated aqueous CuCl (pH 1.5) with 10 ml of aqueous samples with different pH values (−1.1, 2.5, 4.3, 6.5 and 8.5). Inset shows the corresponding optical images of the resultant products.

After adding a solution with pH = 6.5, the initially dark-green solution became yellowish after several minutes (see the inset in Fig. 2), and its spectrum (orange line in Fig. 2) exhibited a step-like absorption, typical of a semiconductor with an absorption edge around 600 nm that corresponds to the band gap of $Cu_2O$.[24] Finally, upon adding a solution with pH = 8.5, the mixture turned orange (see the inset in Fig. 2), and the deposit only exhibited the absorption edge of $Cu_2O$, while that of CuCl disappeared. The TEM image of the deposit from this sample (Fig. S3c†) shows numerous $Cu_2O$ NCs with sizes ranging from 20 to 100 nm and with a single-crystalline structure (Fig. S3d†). These results imply that the alkaline hydrolysis indeed proceeds at a pH above 5.0, resulting in $Cu_2O$ according to eqn (3). The experimental results thus lend support to the above mentioned pH boundary values that separate the reactions in eqn (1)–(3).

In the present work, the conversion of CuCl micro-powder to uniform hollow $Cu_2O$ NCs was designed based on the above described behavior of CuCl in water media with different pH values. First, we took advantage of the pH-controlled complexation and precipitation reactions of CuCl micro-powder at very low pH values (eqn (1)) to prepare uniform CuCl NCs. Next, the pH was raised to an appropriate value (6.5) at which the alkaline hydrolysis reaction could proceed, converting the as-prepared uniform CuCl NCs (serving as sacrificial templates) into hollow $Cu_2O$ NCs, according to eqn (3).

The above outlined synthetic strategy was proved to be feasible by our experimental results. To obtain uniform CuCl NCs, CuCl micro-powder was first dissolved in aqueous HCl with a very low pH value of 0.5, giving a $HCuCl_2$ solution according to eqn (1). Then the pH value of the solution was increased to 6.5 by adding pure water. As a result, the reverse reaction (*i.e.* CuCl precipitation) could proceed at very high rates, leading to uniform CuCl NCs formed *via* quick and homogenous nucleation and growth, as shown in Fig. 3a and

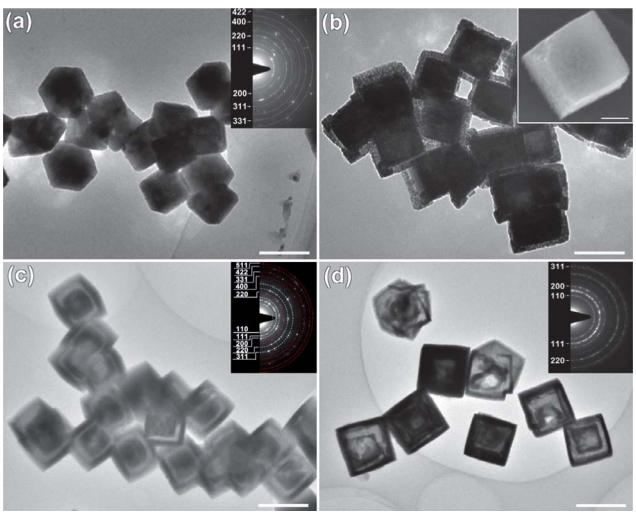


**Fig. 3** TEM images demonstrating a gradual conversion of CuCl NCs to hollow $Cu_2O$ NCs at a pH of 6.5. The hydrolysis evolution is shown after 0 (a), 10 (b), 20 (c), and 30 min (d). The scale bars are 200 nm. The insets in panels (a), (c) and (d) are the corresponding SAED patterns of the TEM images, while the inset in panel (b) is an SEM image of a CuCl nanocube after 10 min of hydrolysis, where the scale bar is 100 nm.

 

S4a.† The selective area electron diffraction (SAED) pattern (inset in Fig. 3a) and the XRD pattern in Fig. S4b† confirm that the NCs are cubic CuCl.

As the medium pH was high enough (6.5), the as-precipitated CuCl NCs were subject to alkaline hydrolysis (according to eqn (3)) which gradually proceeded, producing hollow $Cu_2O$ NCs. As shown in Fig. S5,† the XRD peaks related to $Cu_2O$ gradually merged and grew with reaction time, suggesting a gradual formation of $Cu_2O$ as the result of alkaline hydrolysis. To track the morphological evolution during this stage, we collected CuCl NCs that quickly formed upon adding pure water using a nickel TEM grid, dipped the grid in water with a pH of 6.5 for different lengths of time, and then observed them by means of TEM (see Fig. 3). At the very beginning of the hydrolysis (2 min), separated $Cu_2O$ nanoparticles formed on the surface of the CuCl NCs (see Fig. S6a and b†). The number of $Cu_2O$ nanoparticles increased with reaction time, and they gradually connected into a layer at 5 min (Fig. S6c and d†). After 10 min of hydrolysis, CuCl–$Cu_2O$ core–shell NCs were found in the product (Fig. 3b). The $Cu_2O$ shells are seen to be porous at this stage (inset in Fig. 3b). After 20 min of hydrolysis, the product morphology is rather that of a yolk–shell type, and the shells become more compact (Fig. 3c). As expected, the $Cu_2O$ diffraction pattern emerged in the SAED pattern (inset in Fig. 3c). After 30 min of hydrolysis, hollow $Cu_2O$ NCs were formed, some of them demonstrating double shells (Fig. 3d). The SAED pattern shown in the inset of Fig. 3d confirms that the hollow NCs are composed of nearly pure $Cu_2O$.

The hollow $Cu_2O$ NCs prepared *via* the above described process possess surfaces free of any surfactants or modifiers. Therefore they can be bound with organic molecules to form functional complexes. Although $Cu_2O$ is regarded as a possible luminescent material,[44,45] light emission has been seldom observed for $Cu_2O$ nanostructures prepared so far.[23,31] At the same time, $Cu_2O$ nanomaterials capped with PVP were reported to serve as a photocatalyst to degrade rhodamine B (RhB) molecules and bleach their light emission under UV/Vis irradiation.[31] Surprisingly, the hollow $Cu_2O$ NCs obtained in the present work exhibited a strong luminescent peak at 490 nm (see Fig. 4a), which is believed to originate from the band edge emission from the $\Gamma^+$ to the sub-levels created by the interaction of two excitons, or the $^3D$–$^1D$ splitting in $Cu^+$ ($3d^94s^2$).[46,47] After the as-prepared hollow $Cu_2O$ NCs were mixed with RhB, the luminescent intensity of the latter increased gradually with irradiation time under a 365 nm UV lamp (see Fig. 4b), which has not yet been reported in the literature. In contrast, the luminescence of pure RhB was bleached by irradiation with the same UV lamp (Fig. 4b).

The observed luminescence enhancement of RhB might arise from two possible mechanisms, *i.e.* from the electron transfer and/or the Förster resonance energy transfer (FRET) from the hollow $Cu_2O$ NCs to RhB. The lowest unoccupied molecular orbital (LUMO) level of RhB was reported to be at about −2.2 eV,[48] which is much higher than the conduction band edge of $Cu_2O$ (−3.6 eV).[49] This makes the former mechanism invalid for the luminescence enhancement of RhB. On the other hand, the luminescent peak of the hollow $Cu_2O$ NCs is clearly seen in Fig. 4

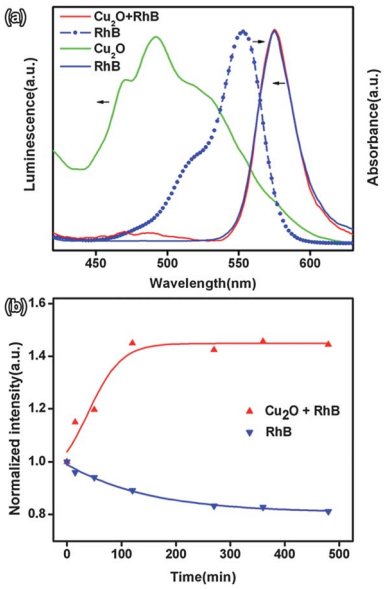


**Fig. 4** Optical properties of hollow $Cu_2O$ NCs, RhB, and their mixture. (a) Luminescence spectra of hollow $Cu_2O$ NCs, RhB, and their mixture irradiated by a 365 nm UV lamp, as well as absorption spectrum of RhB. (b) Normalized plots of the luminescence intensity *versus* irradiation time under a UV lamp with a wavelength of 365 nm. ▼ and ▲ denote RhB and its mixture with hollow $Cu_2O$ NCs, respectively. The lines are given only as a guide to the eye.

to cover the absorption band of RhB, which implies that the energy transfer is feasible for the $Cu_2O$–RhB system.

Because of the surfactant-free preparation process, the hollow $Cu_2O$ NCs are believed to possess clean surfaces capable of adsorbing and binding RhB molecules through their dangling N bonds. The Fourier transform infrared (FTIR) spectroscopy results shown in Fig. S6† confirm this assumption. RhB molecules exhibit an antisymmetric stretching vibration peak of imine at 2360 $cm^{-1}$, a symmetric stretching vibration peak of imine at 1646 $cm^{-1}$, and an absorption peak of carbonyl groups at 1695 $cm^{-1}$. After the RhB solution was added to the hollow $Cu_2O$ NCs, the antisymmetric stretching vibration peak of imine groups disappeared, and the symmetric stretching vibration peak of imine groups moved to 1651 $cm^{-1}$, which was accompanied by a decrease in its intensity. Simultaneously, the absorption peak of carbonyl groups shifted to 1715 $cm^{-1}$ and its intensity became weak. The observed changes in the FTIR peaks indicate that the RhB molecules bind to the hollow $Cu_2O$ NCs through their imine and carbonyl groups. This leads to an enrichment of RhB molecules around the hollow $Cu_2O$ NCs and significantly decreases the distance between the two components. As a result, the FRET from the $Cu_2O$ to RhB is facilitated, thus remarkably enhancing the luminescence of RhB.

## Conclusions

Well-shaped hollow $Cu_2O$ NCs with a narrow size distribution have been efficiently produced *via* a hydrolysis method. In the proposed one-pot method, CuCl micro-powder was first dissolved in aqueous HCl with a very low pH value, after which uniform CuCl NCs precipitated upon adding pure water and thus raising

pH value to 6.5. As the final step, the as-prepared fine CuCl NCs then gradually reacted with water, giving rise to uniform hollow $Cu_2O$ NCs as a result of full hydrolysis. This is the first report on the synthesis of hollow $Cu_2O$ NCs without any reductants or surfactants involved. Importantly, the described synthetic route is not only a simple way to produce hollow $Cu_2O$ NCs, but it also uses low-cost chemicals, and thus can be easily scaled up. In addition, the as-prepared hollow nanomaterials exhibit extraordinary optical properties, which make them attractive for potential applications in photocatalytic and photovoltaic fields.

## Experimental section

To investigate the behavior of CuCl at different pH levels, aqueous solutions with different pH values (−1.1, 2.5, 4.3, 6.5, and 8.5) and 10 ml in volume each were first prepared using HCl or NaOH. CuCl micro-powder from J&K Chemical Co., Ltd. was dissolved in aqueous HCl with a pH value of 0.5 to obtain a saturated solution at room temperature. Then the solutions with different pH values were each added to 0.1 ml of the prepared saturated solution and kept at room temperature for 0.5 h. For instance, to obtain hollow $Cu_2O$ NCs, 10 ml of water with a pH of 6.5 was mixed with 0.1 ml of the saturated CuCl solution (pH 0.5) and reacted for 0.5 h at room temperature.

The impact of the hollow $Cu_2O$ NCs on the luminescence of RhB was investigated under UV irradiation with a wavelength of 365 nm. 2.5 ml of the $Cu_2O$ nanomaterial suspension in water obtained at pH 6.5 and 0.5 ml of aqueous RhB solution were mixed. After remaining non-agitated for 15 min, the mixture was exposed to photoirradiation.

The morphology and structure were determined by scanning electron microscopy (SEM, Hitachi S-4800) and transmission electron microscopy (TEM, FEI Technai G2 F20), the latter instrument being equipped with a field emission gun and an energy-dispersive X-ray spectroscopy (EDS) unit. Absorption spectra were recorded with a Hitachi U-3010 spectrometer. X-ray diffraction (XRD) patterns were collected on a Rigaku D/max 2500v/pc diffractometer. Fourier transform infrared (FTIR) analysis was performed using a Bruke Tensor 27 spectrometer. The luminescence was measured by a Hitachi F-4500 spectrometer.

## Acknowledgements

This work was supported by the Natural Science Foundation of China (no. 51102176, 50972102 and 50902103), the National High-tech R&D Program of China (no. 2009AA03Z301), and the Natural Science Foundation of Tianjin City (no. 11JCYBJC02000, 09JCZDJC22600 and 08JCYBJC02900).

## Notes and references

1 X. W. Lou, L. A. Archer and Z. Yang, *Adv. Mater.*, 2008, **20**, 3987–4019.
2 B. Wang, J. S. Chen, H. B. Wu, Z. Y. Wang and X. W. Lou, *J. Am. Chem. Soc.*, 2011, **133**, 17146–17148.
3 L. Zhou, D. Zhao and X. Lou, *Angew. Chem., Int. Ed.*, 2012, **51**, 239–241.
4 L. Zhou, D. Zhao and X. W. Lou, *Adv. Mater.*, 2012, **24**, 745–748.
5 K. Y. Niu, J. Yang, S. A. Kulinich, J. Sun and X. W. Du, *Langmuir*, 2010, **26**, 16652–16657.
6 K. Y. Niu, J. Yang, J. Sun and X. W. Du, *Nanotechnology*, 2010, **21**, 295604.
7 K. Y. Niu, J. Yang, S. A. Kulinich, J. Sun, H. Li and X. W. Du, *J. Am. Chem. Soc.*, 2010, **132**, 9814–9819.
8 C. Su, H. Wang and X. Liu, *Cryst. Res. Technol.*, 2011, **46**, 209–214.
9 W. W. Wang and J. L. Yao, *Mater. Res. Bull.*, 2010, **45**, 1672–1678.
10 J. S. Chen, C. Chen, J. Liu, R. Xu, S. Z. Qiao and X. W. Lou, *Chem. Commun.*, 2011, **47**, 2631–2633.
11 Y. Liu, L. Yu, Y. Hu, C. F. Guo, F. M. Zhang and X. W. Lou, *Nanoscale*, 2012, **4**, 183–187.
12 Y. Piao, A. Burns, J. Kim, U. Wiesner and T. Hyeon, *Adv. Funct. Mater.*, 2008, **18**, 3745–3758.
13 J. Kim, Y. Piao and T. Hyeon, *Chem. Soc. Rev.*, 2009, **38**, 372–390.
14 L. Zhang, S. Qiao, Y. Jin, Z. Chen, H. Gu and G. Q. Lu, *Adv. Mater.*, 2008, **20**, 805–809.
15 J. Liu, S. B. Hartono, Y. G. Jin, Z. Li, G. Q. Lu and S. Z. Qiao, *J. Mater. Chem.*, 2010, **20**, 4595–4601.
16 D. Deng and J. Y. Lee, *Chem. Mater.*, 2008, **20**, 1841–1846.
17 M. H. Kim, X. Lu, B. Wiley, E. P. Lee and Y. Xia, *J. Phys. Chem. C*, 2008, **112**, 7872–7876.
18 K. An and T. Hyeon, *Nano Today*, 2009, **4**, 359–373.
19 F. Caruso, R. A. Caruso and H. Mohwald, *Science*, 1998, **282**, 1111–1114.
20 D. H. M. Buchold and C. Feldmann, *Nano Lett.*, 2007, **7**, 3489–3492.
21 S. F. Wang, F. Gu and M. K. Lu, *Langmuir*, 2006, **22**, 398–401.
22 X. Yu, C. Cao, H. Zhu, Q. Li, C. Liu and Q. Gong, *Adv. Funct. Mater.*, 2007, **17**, 1397–1401.
23 L.-I. Hung, C.-K. Tsung, W. Huang and P. Yang, *Adv. Mater.*, 2010, **22**, 1910–1914.
24 B. D. Yuhas and P. Yang, *J. Am. Chem. Soc.*, 2009, **131**, 3756–3761.
25 C. Malerba, F. Biccari, C. L. A. Ricardo, M. D'Incau, P. Scardi and A. Mittiga, *Sol. Energy Mater. Sol. Cells*, 2011, **95**, 2848–2854.
26 S. Nikitine, J. B. Grun and M. Sieskind, *J. Phys. Chem. Solids*, 1961, **17**, 292–300.
27 W. Septina, S. Ikeda, M. A. Khan, T. Hirai, T. Harada, M. Matsumura and L. M. Peter, *Electrochim. Acta*, 2011, **56**, 4882–4888.
28 K. Akimoto, S. Ishizuka, M. Yanagita, Y. Nawa, G. K. Paul and T. Sakurai, *Sol. Energy*, 2006, **80**, 715–722.
29 V. Georgieva and M. Ristov, *Sol. Energy Mater. Sol. Cells*, 2002, **73**, 67–73.
30 M. Hara, T. Kondo, M. Komoda, S. Ikeda, K. Shinohara, A. Tanaka, J. N. Kondo and K. Domen, *Chem. Commun.*, 1998, 357–358.
31 Y. Sui, W. Fu, Y. Zeng, H. Yang, Y. Zhang, H. Chen, Y. Li, M. Li and G. Zou, *Angew. Chem., Int. Ed.*, 2010, **49**, 4282–4285.

 

32 C. H. Lu, L. M. Qi, J. H. Yang, X. Y. Wang, D. Y. Zhang, J. L. Xie and J. M. Ma, *Adv. Mater.*, 2005, **17**, 2562–2567.
33 J. J. Teo, Y. Chang and H. C. Zeng, *Langmuir*, 2006, **22**, 7369–7377.
34 L. Zhang and H. Wang, *ACS Nano*, 2011, **5**, 3257–3267.
35 P. D. Cozzoli, A. Kornowski and H. Weller, *J. Am. Chem. Soc.*, 2003, **125**, 14539–14548.
36 F. Bosc, A. Ayral, P. A. Albouy and C. Guizard, *Chem. Mater.*, 2003, **15**, 2463–2468.
37 M. S. Kharasch and P. O. Tawney, *J. Am. Chem. Soc.*, 1941, **63**, 2308–2316.
38 J. T. B. H. Jasrzebski and G. V. Koten, in *Modern Organocopper Chemistry*, ed. N. Krause, Wiley-VCH, Weinheim, Germany, 2002, p. 1.
39 J. J. Fritz, *J. Phys. Chem.*, 1980, **84**, 2241–2246.
40 Y. Shang, D. F. Zhang and L. Guo, *J. Mater. Chem.*, 2012, **22**, 856–861.
41 N. N. Greenwood and A. Earnshaw, *Chemistry of the Elements*, Butterworth-Heinemann, Oxford, UK, 2nd edn, 1997.
42 D. B. Pedersen, S. Wang and S. H. Liang, *J. Phys. Chem. C*, 2008, **112**, 8819–8826.
43 Q. Darugar, W. Qian, M. A. El-Sayed and M. P. Pileni, *J. Phys. Chem. B*, 2006, **110**, 143–149.
44 P. Sharma and H. S. Bhatti, *Mater. Chem. Phys.*, 2009, **114**, 889–896.
45 Z. Yang, C. K. Chiang and H. T. Chang, *Nanotechnology*, 2008, **19**, 025604.
46 R. J. Elliott, *Phys. Rev.*, 1961, **124**, 340–345.
47 P. Sharma and H. S. Bhatti, *Mater. Chem. Phys.*, 2009, **114**, 889–896.
48 X. Chang, M. A. Gondal, A. A. Al-Saadi, M. A. Ali, H. Shen, Q. Zhou, J. Zhang, M. Du, Y. Liu and G. Ji, *J. Colloid Interface Sci.*, 2012, **377**, 291–298.
49 C. X. Xiang, G. M. Kimball, R. L. Grimm, B. S. Brunschwig, H. A. Atwater and N. S. Lewis, *Energy Environ. Sci.*, 2011, **4**, 1311–1318.